Finite element modeling of dynamics of martensitic phase transitions

Alexander V. Idesman,[a] Joon-Yeoun Cho, and Valery I. Levitas
Department of Mechanical Engineering, Texas Tech University, Lubbock, Texas 79409, USA

(Received 27 February 2008; accepted 14 June 2008; published online 28 July 2008)

A finite element approach is suggested for the modeling of the dynamics of multivariant martensitic phase transitions (PTs) in elastic materials at the nanoscale in the three dimensional (3D) case. The model consists of a coupled system of the Ginzburg–Landau equations for transformation strain-related order parameters and dynamic elasticity equations. Thermodynamic potential [V. Levitas and D. Preston, Phys. Rev. B **66**, 134206 (2002)] that captures the main features of macroscopic stress-strain curves is used. The evolution of multivariant microstructure in a 3D specimen for cubic to tetragonal PT in a NiAl alloy is modeled with dynamic and static formulations. The numerical results show the significant influence of inertial forces on microstructure evolution. © *2008 American Institute of Physics*. [DOI: 10.1063/1.2955514]

For the simulation of microstructure evolution during martensitic (diffusionless first-order) PT at the nanoscale, phase field or Ginzburg–Landau approaches are used (see Refs. 1–10). The papers based on these techniques differ in the choice of (a) the order parameters (selected strain components or transformation strain-related variables) that describe the evolution of each martensitic variant; (b) thermodynamic potential; (c) total number of equations (additional kinetic equations for the order parameters are introduced if the order parameters are the transformation strain-related variables); (d) variables, the rate of which determines the dissipation rate; (e) elastostatic or elastodynamic formulations, and (g) numerical approaches. In all the papers,[1–10] spectral methods were used for numerical simulations of the microstructure evolution. In Refs. 9 and 10, the dynamic formulation with inertial forces suggested in Refs. 5 and 6 was applied for the simulation of two dimensional and three dimensional (3D) microstructures at phase transition (PT). Theories in Refs. 5, 6, 9, and 10 are based on the order parameters consisting of the selected strain components with a Rayleigh dissipative function expressed in terms of strain rates. Such an approach results in the appearance of viscous stresses and viscoelastic constitutive equations. We are not aware of simulations based on dynamic formulations for the transformation strain-related order parameters.

Recently, we made several steps toward more realistic modeling of stress-induced martensitic transformations. Some of these steps are independent of the development in the current paper. (1) Surface effect was studied in Ref. 11. (2) A thermal resistance to the interface propagation was introduced in Ref. 12. (3) The phase-field approach was extended for the microscale in Refs. 13 and 14. More importantly, an advanced thermodynamic potential was developed[15,16] that can describe the typical stress-strain curves observed experimentally, all the temperature-dependent thermomechanical properties of austenite and martensitic variants, and PT between austenite and martensitic variants, and between martensitic variants with arbitrary types of symmetry. The potential was based on the transformation strain-related order parameters.

In the paper we suggest a phase-field approach for martensitic PT that has the following features.

- The advanced expression for the free energy suggested in Refs. 15 and 16 is used, which in contrast to known approaches,[1–10] correctly describes the main experimental features of stress-induced PT.
- The elastodynamics equations are used which has not been done before for theories based on transformation strain-related order parameters.
- Dissipation rate is determined by the rate of the order parameters, which results in the time-dependent Ginzburg–Landau (TDGL) equations; viscous stresses are not used.
- A finite element approach to the solution of the 3D-coupled elastodynamics and TDGL equations is developed. Since the equations for the order parameters are similar to the heat transfer equation, the total system of equations for the modeling of PT is similar to the system of coupled thermoelasticity and heat transfer equations.

Based on the phase-field approach developed, the simulation of microstructure evolution for cubic-tetragonal martensitic PT in a NiAl alloy is presented for statics (without inertial forces) and dynamics (with inertial forces) in the 3D case. The numerical results show the very significant influence of inertial effects on microstructure evolution, even for the traditional problem on relaxation of initial perturbations to stationary microstructure.

Multivariant martensitic microstructure may consist of austenite and n martensitic variants, and can be represented in terms of the distribution of n order parameters η_k ($k=1,2,\ldots,n$). The order parameters η_k in the current approach vary from zero to unity, where $\eta_k=1$ corresponds to the kth martensitic variant and $\eta_i=0$ for all i corresponds to austenite. The following system of equations is used for the modeling of martensitic PT at nanoscale: relationship between strains ε_{ij} and displacements u_i

$$\varepsilon_{ij}=0.5(u_{i,j}+u_{j,i}), \tag{1}$$

Hooke's law

$$\varepsilon_{mk}= =-\partial G/\partial\sigma_{mk}=\lambda_{ijmk}\sigma_{ij}+\varepsilon^t_{mk}, \tag{2}$$

equations of motion

$$\sigma_{ij,i}=\rho\ddot{u}_j, \tag{3}$$

and the Ginzburg–Landau kinetic equations

[a]Electronic mail: alexander.idesman@coe.ttu.edu.

$$\frac{\partial \eta_k}{\partial t} = -L\frac{\delta \bar{G}}{\delta \eta_k} = L\beta\left(\frac{\partial^2 \eta_k}{\partial x_1^2} + \frac{\partial^2 \eta_k}{\partial x_2^2} + \frac{\partial^2 \eta_k}{\partial x_3^2}\right) - L\frac{\partial G}{\partial \eta_k}, \quad k = 1,2,\ldots,n, \tag{4}$$

where $\varepsilon_{ij}^t(\eta_k)$ is the transformation strain tensor, σ_{ij} is the stress tensor, λ_{ijmn} is the elastic compliance tensor, ρ is the mass density, L and β are the material parameters, G is the thermodynamic potential, $\bar{G}=G+0.5\beta\eta_{n,i}\eta_{n,i}$, and $\delta/\delta\eta_k$ is the variational derivative.

One of the critical points of the theory is the choice of the thermodynamic potential G. We will use the following potential $G(\sigma_{mn},\theta,\eta_i)$ suggested in Ref. 15, which captures the main features of macroscopic stress-strain curves and meets the experimental data:

$$G = -\sigma_{ij}\lambda_{ijmn}\sigma_{mk} - \sigma_{mk}\varepsilon_{mk}^t + \sum_{k=1}^{n}[A\eta_k^2 + (4\Delta G^\theta - 2A)\eta_k^3 + (A - 3\Delta G^\theta)\eta_k^4] + F(\eta_1,\eta_2,\ldots,\eta_n), \tag{5}$$

$$\varepsilon_{mk}^t = \sum_{i=1}^{n}\bar{\varepsilon}_{mk}^i[a\eta_i^2 + (4-2a)\eta_i^3 + (a-3)\eta_i^4], \tag{6}$$

where

$$\Delta G^\theta = A_0(\theta-\theta_e)/3, \quad A = A_0(\theta-\theta_c)/3, \tag{7}$$

$$F(\eta_1,\eta_2,\ldots,\eta_n) = \sum_{i=1}^{n-1}\sum_{j=i+1}^{n}F_{ij}(\eta_i,\eta_j), \tag{8}$$

$$F_{ij} = \eta_i\eta_j(1-\eta_i-\eta_j)\{B[(\eta_i-\eta_j)^2 - \eta_i - \eta_j] + D\eta_i\eta_j\} + \eta_i^2\eta_j^2(\eta_i Z_{ij} + \eta_j Z_{ji}), \tag{9}$$

$$Z_{ij} = \bar{A} - A + \sigma_{mk}[(a-3)\bar{\varepsilon}_{mk}^j + 3\bar{\varepsilon}_{mk}^i]. \tag{10}$$

Here θ_e, θ_c, a, A_0, $\bar{A}$, B, D are material parameters, θ is the temperature, and $\bar{\varepsilon}_{mk}^i$ $(i=1,2,\ldots,n)$ is the transformation strain tensor for the ith martensitic variant (known from crystallography). A temperature evolution equation can be easily added and treated [since the heat transfer equation has a structure similar to that of Eq.(4)]. However, to focus on the effect of advanced potential [Eq.(5)], inertia [Eq. (3)], and the finite element approach, we assume isothermal approximation (as in all previous works[1–14]).

Let us analyze a system of Eqs.(1)–(4). Equations (1)–(3) resemble standard elastodynamics equations if the transformation strain ε_{mk}^t is treated as the thermal strain. Equation (4) is similar to nonstationary heat transfer equations. For $n=1$, we have an analog of a standard system of coupled heat transfer and elastodynamics equations. For $n>1$, we have a system similar to coupled n heat transfer equations and elastodynamics equations. Coupling follows from the fact that the transformation strain ε_{mk}^t in the elastodynamics equations depends on the order parameters η_i; and the term $\partial G/\partial\eta_i$ in Eq. (4) depends on the stress σ_{mk}. For neglected inertial forces (i.e., $\rho\ddot{u}_j=0$), Eq. (3) reduces to the mechanical equilibrium equation (the static formulation).

To solve Eqs. (1)–(4), the finite element method is used. For the integration of the system of equations in time, the total observation time is subdivided into N time steps with the small time increments Δt. Then in order to find unknown parameters at the end of each time step, we assume that (a) for the kth Eq. (4), the order parameters η_m $(m=1,2,k-1,k+1,\ldots,n)$ and stresses are fixed and known from the previous time step; (b) for Eqs. (1)–(3), all order parameters are fixed and known from the previous solution of Eqs. (4). These assumptions correspond to an explicit time integration scheme and allow the decoupling of the system [Eqs. (1)–(4)] at any small time step; i.e., any kth [Eq. (4)] and system [Eqs. (1)–(3)] can be solved separately. For the solution to the kth [Eq. (4)] and system [Eqs. (1)–(3)] at any time step, the finite element algorithms with an implicit time integration method for heat transfer problems and elasticity problems are applied, respectively. The algorithm is implemented into the finite element program "FEAP" (Ref. 17) for the general 3D case. The finite element method is well developed for elasticity and heat transfer equations and can easily be applied to complicated geometry, boundary and initial conditions, and heterogeneous materials.

Let us consider the modeling of microstructure for cubic-tetragonal martensitic PT in a NiAl alloy with three martensitic variants using the static formulation (without inertial forces) and a more general dynamic formulation (with inertial forces) in the 3D cases. A standard problem on relaxation of initial stochastic perturbations into stationary martensitic microstructure is solved to demonstrate the importance of inertia even for the case when not much is expected (e.g., in contrast to shock loading). The following material parameters that adequately describe the stress-strain curve for martensitic PT in a NiAl alloy are used (see Ref. 15): $a=2.98$; $\bar{A}=5320$ MPa; $\theta_e=215$ K; $\theta_c=-183$ K; $A_0=4.4$ MPa/K; $B=0$; $D=500$ MPa; $\beta=2.33\times10^{11}$ N; $L=2596.5$ m^2/N s; $\bar{\varepsilon}_{11}^1=0.215$; $\bar{\varepsilon}_{22}^1=-0.078$; $\bar{\varepsilon}_{33}^1=-0.078$; $\bar{\varepsilon}_{11}^2=-0.078$; $\bar{\varepsilon}_{22}^2=0.215$; $\bar{\varepsilon}_{33}^2=-0.078$; $\bar{\varepsilon}_{11}^3=-0.078$; $\bar{\varepsilon}_{22}^3=-0.078$; $\bar{\varepsilon}_{33}^3=0.215$; $\bar{\varepsilon}_{ij}^1=\bar{\varepsilon}_{ij}^2=\bar{\varepsilon}_{ij}^3=0$ for $i\neq j$; $E=198\,300$ MPa; $\nu=0.33$; and $\rho=5850$ kg/m^3. Here E is Young's modulus and ν is Poisson's ratio (the elastic modulus tensor $\boldsymbol{C}$ is assumed for simplicity to be isotropic and phase independent). A cubic specimen with dimension $25\times25\times25$ nm was considered. The initial conditions for the system [Eqs. (1)–(4)] were as follows: (a) the initial random distribution of the order parameters η_1, η_2, and η_3 with values between 0 and 1 was given; (b) initial displacements and velocities (for the dynamic case only) were zero for the whole specimen; and (c) homogeneous initial stresses ($\sigma_{11}^{in}=\sigma_{22}^{in}=\sigma_{33}^{in}=2$ GPa and $\sigma_{12}^{in}=\sigma_{23}^{in}=\sigma_{13}^{in}=0$) were applied to the whole specimen for the promotion of PT. The boundary conditions for the elastic problem [Eqs. (1)–(3)] were as follows: $u_n=0$ and $\tau_n=0$, where u_n and τ_n are the normal displacements and the tangential stresses, respectively. The boundary conditions for Eq. (4) were prescribed as zero fluxes $\partial\eta_i/\partial n=0$ along the whole boundary of the specimen. We also assumed the homogeneous temperature $\theta=288$ K, which does not change during PT. The observation time $\tilde{t}=4.2\times10^{-10}$ s at which the microstrucure became practically stationary, was subdivided into 14 000 time steps. The evolution of microstructures for the static and dynamic formulations is shown in Fig. 1. Let us compare the solutions obtained. The evolution rate of a microstructure for the static formulation is much faster than that for the dynamic formulation, e.g., as we can see from column 1 in Fig. 1, the randomly distributed initial order parameters form micro-

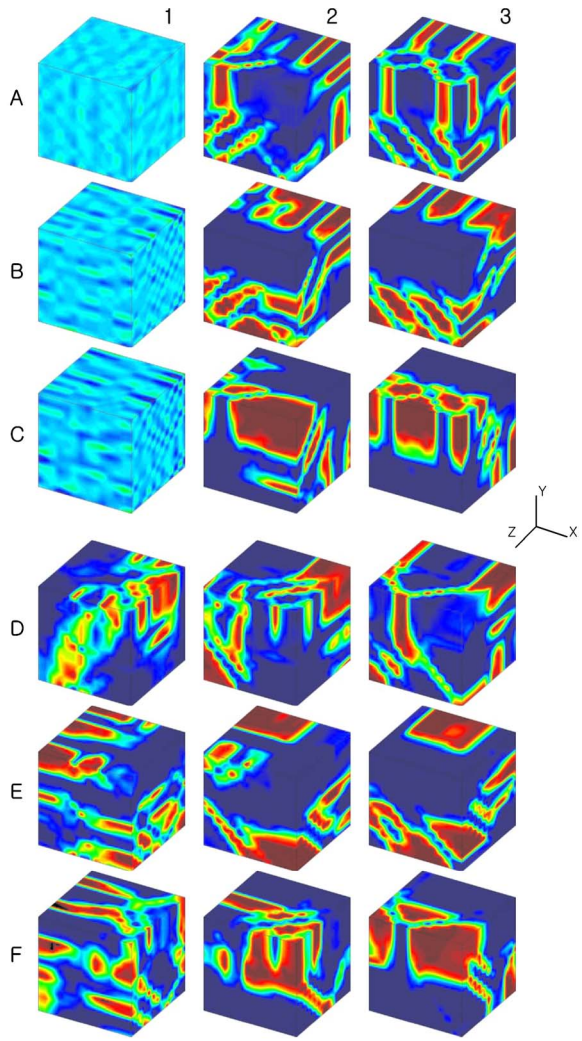

FIG. 1. (Color online) Evolution of microstructure in the 3D specimen. Rows A–C and D–F are the evolution of the microstructure (the order parameters) obtained as solutions of dynamic and static problems, respectively. Rows A and D are for variant 1, rows B and E are for variant 2, and rows C and F are for variant 3. Columns 1–3 are the temporal sequences for time T of 1.5×10^{-12}, 4.8×10^{-11}, and 4.2×10^{-10} s, respectively. In each sample, red represents each martensitic variant and blue represents the other two martensitic variants, or austenite.

structure with several martensitic plates in the static formulation at time $t=1.5\times10^{12}$ s. However, at the same time, there is no martensitic microstructure for the dynamic formulation, i.e., only intermediate values between 0 and 1 of the order parameters occur in the whole specimen. Next, for the static and dynamic formulations, the corresponding microstructures have different evolution histories. Finally, the microstructures at the final time considered are totally different; see column 3 in Fig. 1.

Figure 2 shows the schematic of the martensitic microstructure for the dynamic case at the final time instant, which contains all three martensitic variants in one picture. The sample is divided into several regions consisting of two martensitic variants in twin relations. Planes between twin-related variants are designated in Fig. 2 and coincide with those determined from the crystallographic theory.

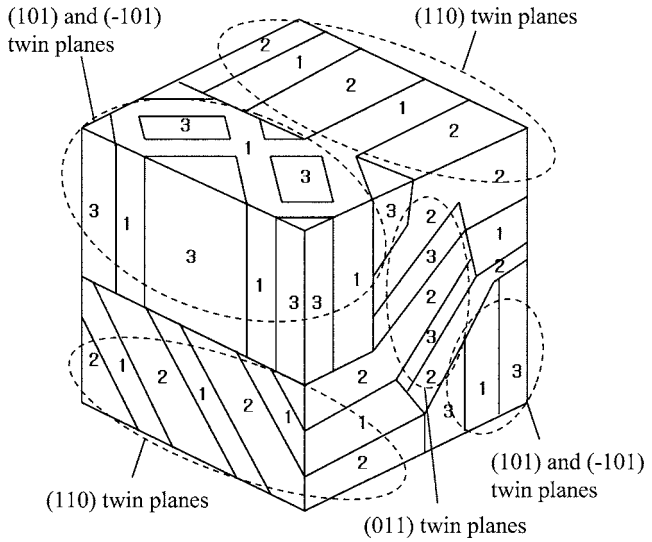

FIG. 2. Schematic of martensitic microstructure for the dynamic formulation at the final time instant, which contains all three martensitic variants. The sample is divided into several regions consisting of two martensitic variants in twin relations. Designated planes between the twin-related variants coincide with those determined from the crystallographic theory.

In summary, an advanced dynamics formulation for the modeling of stress-induced martensitic PT is suggested. The finite element approach is applied to the solution of 3D-coupled elastodynamics and phase-field equations. The numerical results show the essential effect of inertial forces on the evolution and the formation of the final martensitic microstructure.

The research of A.V.I. was supported in part by the Texas Higher Education Coordinating Board under Grant No. 003644 0008 2006 and DOE under Grant No. DE-FC03-03NA00144. V.I.L. acknowledges support of NSF (CMS-0555909 and CBET-0755236) and ONR (N000140810104).

[1] Y. Wang and A. Khachaturyan, Acta Mater. **45**, 759 (1997).
[2] T. Ichitsubo, K. Tanaka, M. Koiwa, and Y. Yamazaki, Phys. Rev. B **62**, 5435 (2000).
[3] A. Artemev, Y. Jin, and A. Khachaturyan, Acta Mater. **49**, 1165 (2001).
[4] D. Seol, S. Hu, Y. Li, L. Chen, and K. Oh, Met. Mater. Int. **9**, 221 (2003).
[5] S. Curnoe and A. Jacobs, Phys. Rev. B **63**, 094110 (2001); **64**, 064101 (2001).
[6] A. Jacobs, S. Curnoe, and R. Desai, Phys. Rev. B **68**, 224104 (2003).
[7] S. Shenoy, T. Lookman, A. Saxena, and A. Bishop, Phys. Rev. B **60**, R12537 (1999).
[8] K. Rasmussen, A. Saxena, A. Bishop, R. Albers, and S. Shenoy, Phys. Rev. Lett. **87**, 055704 (2001).
[9] T. Lookman, S. Shenoy, K. Rasmussen, A. Saxena, and A. Bishop, Phys. Rev. B **67**, 024114 (2003).
[10] T. Lookman, S. Shenoy, K. Rasmussen, A. Saxena, and A. Bishop, J. Phys. IV **112**, 195 (2003).
[11] V. Levitas, D.-W. Lee, and D. Preston, Europhys. Lett. **76**, 81 (2006).
[12] V. Levitas and D.-W. Lee, Phys. Rev. Lett. **99**, 245701 (2007).
[13] V. Levitas, A. Idesman, and D. Preston, Phys. Rev. Lett. **93**, 105701 (2004).
[14] A. Idesman, V. Levitas, D. Preston, and J.-Y. Cho, J. Mech. Phys. Solids **53**, 495 (2005).
[15] V. Levitas and D. Preston, Phys. Rev. B **66**, 134206 (2002).
[16] V. Levitas, D. Preston, and D.-W. Lee, Phys. Rev. B **68**, 134201 (2003).
[17] O. Zienkiewicz and R. Taylor, *The Finite Element Method* (Butterworth-Heinemann, Oxford, UK, 2000).